Steady State Thermo XFEM Fracture Analysis of Isotropic and an Isotropic FG Plate with Inclined Center Crack

Dr. Hassanein Ibraheem Khalaf
Mech. Engineering Dept
University of Basrah
Basrah
hassanein.ibraheem@gmail.com

Dr. Haider Khazal Mehbes
Mech. Engineering Dept
University of Basrah
Basrah
haider_khazal@yahoo.ccom

Dr. Ameen Ahmed Nassar
Mech. Engineering Dept
University of Basrah
Basrah
aaledani@gmail.com

Abstract-**The extended-finite element method (X-FEM) is used for crack analysis of orthotropic and isotropic functionally-graded composite material (FGCM) plate with slanted crack under thermal loadings. The enrichments functions of discontinuity are implemented. Mixed-mode SIFs are calculated in isotropic and orthotropic FGMs. Gaussian technique (Q4) has been applied in numerical calculation of interaction of solution. Thermal effects, fundamental equations, the interaction integral of non-homogeneous cases (M-integral), and proposal numerical integration rule are set to simulate and to debate the accuracy of the present work results in comparing with the results of the references that available in the literature. In addition, the effect of size of crack is studied to discuss the values of energy release rate and stress intensity factors with different crack angles. The present study is implemented by using MATLAB program to present steady state thermo XFEM fracture analysis of isotropic and an isotropic FG plate with inclined center crack.**

Keywords: **XFEM, orthotropic (anisotropic) and isotropic functionally-graded composite material (FGCM), thermal load, stress intensity factors**

1. INTRODUCTION

Evolution of technology and science in the contemporary time has generated up-to-date challenges for scientists and engineers by applying modern materials. Need to use accession for model of difficult trait in the relevant cases is of a desired significance, principally at status of different mechanical and thermic loadings. Steel or other related homogenous cases can give a good performance under mechanical loads but can be less than its efficiency under the influence of thermal loads while other materials as like ceramics resist the thermal load effects more than the resistance to mechanical loads. The aim of construction of material specifications has put scientists and engineers to product orthotropic and isotropic functionally graded materials (FGMs) and composite materials. FGMs are progressively replacing composite materials in layers in various applications from high-tech metiers to traditional industrials.

In FGMs, the smooth variable conception in properties as porosity, microstructure, and composition in these related materials, that gives in penchant of different specifications such as impact load and high heat gradients, have extended throughout whole important modern industries that require the provision of related properties [1]. Examples of such material applications include shell casing of rockets, lining materials with shafts, aircraft wings, and modern electronic device connectors.

The study of thermal effects on FGMs is of a great importance for two causes. First, functionally graded materials are influenced by temperature through the process of manufacturing and second, the related materials are often utilized in relevant applications under different thermal gradients. Therefore, research of thermal stresses in FGMs is indispensable. So, heat conduction and related effect conditions are essential in an isotropic and an anisotropic FG cases [2, 3].

Fracture analysis in FGM is studied empirically with various cases such shock force [4, 5], crack growth [6, 7], dynamic fracture [8], bi-material FGMs [9] and crack in thermal barrier coatings [10]. Several researches are done in discontinuity study in FGMs. The biggest part of works for related materials are applied via adopt the numerical techniques instead of theoretic procedures as a result of insufficiency to theoretically solution for such complex cases.

The stress intensity factors computation in an isotropic (changing properties in one direction) and orthotropic (changing properties in two direction) FGMs, the stresses singularities in near of crack-tip suppose themselves of an isotropic materials [11]. Dolbow and Gosz [12] submitted an approach to study of FG cases that representation of approximation crack tip regions coincide these ones of identical materials. Rao and Rahman [13] presented the meshfree method (EFGM) in computing crack terms of homogenous FG cases via using (M) integrals in terms of homogenous and non-homogenous auxiliary terms. Furthermore, Kim and Paulino [14,15] presented expended development on the analysis of fracture of FGMs by using finite element method. Dai et al. [16], Sladek et al. [17], Khazal et al. [18] used meshfree methods for analysis the crack problems in functionally graded materials.

Simultaneously with regard to thermal loads, Hasselman and Youngblood illustrated demeanor of conductivity gradient effect in nonhomogeneous material [19], and the asymptotic field of crack propagation was debated via Abotula et al. [20]. Noda and Jin studied the fracture in FGM in semi finite medium for complete isolated [21], at the same time, Borgi and Erdogan considered the fracture applied partially insulation [22, 23] and cracked FGM is applied partly isolated via supposing heat decrease through regions of crack via Ding and Li [24]. Many researchers studied the thermal fracture parameters for isotropic and orthotropic FGMs by using numerical methods (FEM and XFEM) and new related development techniques [25-29]. Numerically, XFEM is an exquisite technique to model the discontinuity. Extended finite element method is the development of the classic and conventional FEM that applies enhancement functions at specific region by employing properties of partition of unity (PU) and heavy-set functions.

The aim of the current research is to represent the isotropic and anisotropic FGMs with Inclined center crack under thermal loadings by applying XFEM. Gauss quadrature rule (Q4) is applied for numerical interaction rather than using sub-triangulation method that used in [29] to reduce time cost and to remove non-coincide integrated points about crack surfaces and tips with give same level of accuracy. Several lengths to the crack are taken into account to predict the magnitude of fracture energy released. Many of the parameters have been obtaining and presentation in the results to have more inclusive research.

2. CRACK-TIP REGION IN FG CASES

Thermal term (ε^{th}) could be depicted in following equation,

$$\varepsilon^{t} = \varepsilon^{m} + \varepsilon^{th} \tag{1}$$

where ε^{t} and $\varepsilon^{th}$are total, mechanical and strain, respectively. ε^{m} can be expressed in [30]

$$\varepsilon^{m}_{\alpha} = \alpha_{\alpha\beta}\sigma_{\beta} \qquad (\alpha, \beta = 1,2,6) \tag{2}$$

where

$$\varepsilon_1 = \varepsilon_{11}\,, \quad \varepsilon_2 = \varepsilon_{22}\,, \quad \varepsilon_6 = 2\varepsilon_{12} \tag{3}$$

$$\sigma_1 = \sigma_{11}\,, \quad \sigma_2 = \sigma_{22}\,, \quad \sigma_6 = \sigma_{12} \tag{4}$$

hence,

$$\begin{bmatrix} a_{11} & a_{12} & a_{16} \\ a_{12} & a_{22} & a_{26} \\ a_{16} & a_{26} & a_{66} \end{bmatrix} = \begin{bmatrix} s_{1111} & s_{1122} & 2s_{1112} \\ s_{2211} & s_{2222} & 2s_{2212} \\ 2s_{1211} & 2s_{1222} & 4s_{1212} \end{bmatrix} \tag{5}$$

where s_{ijkl} are the components of material compliance tensor.

$$\varepsilon^{m}_{ij} = s_{ijkl}\sigma_{kl} \qquad (i, j, k, l = 1,2,3) \tag{6}$$

for plane strain, $a_{\alpha\beta}$ can replace with

$$\left(a_{ij} - \frac{a_{i3}a_{j3}}{a_{33}}\right) \rightarrow a_{ij} \tag{7}$$

In addition, ε^{th}_{ij} can be written as

$$\begin{Bmatrix} \varepsilon^{th}_{11} \\ \varepsilon^{th}_{22} \\ \varepsilon^{th}_{33} \\ 2\varepsilon^{th}_{12} \end{Bmatrix} = \begin{Bmatrix} \lambda_{11} \\ \lambda_{22} \\ \lambda_{33} \\ \lambda_{12} \end{Bmatrix} \Delta T \tag{8}$$

where λ_{ij} is expressed thermal expansion coefficient term α_{ij} for plane stress states

$$\lambda_{11} = \alpha_{11}\,,\ \lambda_{22} = \alpha_{22}\,,\ \lambda_{33} = \alpha_{33}\ ,\ \lambda_{12} = 0 \tag{9}$$

and for plane strain problems,

$$\lambda_{11} = \nu_{31}\alpha_{33} + \alpha_{11}\,, \quad \lambda_{22} = \nu_{32}\alpha_{33} + \alpha_{22}\,,$$

$$\lambda_{33} = \alpha_{33}\ , \quad \lambda_{12} = 0 \tag{10}$$

3. STRESS INTENSITY FACTORS

3.1. J-integral

Three different formulations are used in the literature access SIFs in FGMs, involving non-equilibrium, non-compatibility, and constant-constitutive-tensor formulations, as suggested via [31-32].At current research, non-compatibility condition is applied for calculating *J*-integral for reason that it demands lower intricate derivatives. The non-compatibility conditions rely upon:

$$\sigma_{ij} = c_{ijkl}(x)\varepsilon^{m}_{kl}\ , \quad \sigma_{ij,j} = 0 \tag{11}$$

$$\varepsilon^{t}_{ij} \neq \frac{1}{2}\left(u_{i,j} + u_{j,i}\right) \tag{12}$$

In terms of the equivalent domain formulation for an arbitrary contour (as shown in Fig. 1), the J-integral can be written as

$$J = \int_A \left(\sigma_{ij}u_{i,1} - w\delta_{1j}\right)q_{,j}dA + \int_A \left(\sigma_{ij}u_{i,1} - w\delta_{1j}\right)_{,j}q\,dA \tag{13}$$

The domain of J integral could be shown in Fig. 1.

In addition, the strain-energy term equals to

$$w = \frac{1}{2}\left(\sigma_{11}\varepsilon^{m}_{11} + \sigma_{22}\varepsilon^{m}_{22} + 2\sigma_{12}\varepsilon^{m}_{12}\right) \tag{14}$$

that could be expressed in plane stress cases

$$w = \frac{1}{2}\left(\sigma_{11}\varepsilon^{m}_{11} + \sigma_{22}\varepsilon^{m}_{22} + \sigma_{33}\varepsilon^{m}_{33} + 2\sigma_{12}\varepsilon^{m}_{12}\right) \tag{15}$$

and in plane strain cases,

$$\varepsilon^{t}_{33} = 0\ \rightarrow \varepsilon^{m}_{33} = -\varepsilon^{th}_{33} = -\alpha_{33}\Delta T \tag{16}$$

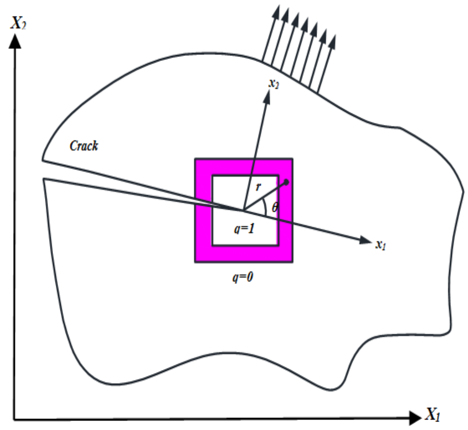

Fig.1 The domain integral.

3.2. Interaction Integral Method

The interaction integral method is adopted for determine modes values of SIFs:

$$J^s = J + J^{aux} + M^l \tag{17}$$

where

$$\sigma_{ij}^{aux}u_{i,1j} = \frac{1}{2}\sigma_{ij}^{aux}\left(u_{i,1j} + u_{j,1i}\right) = \sigma_{ij}^{aux}\varepsilon_{ij,1}^{t} = \sigma_{ij}^{aux}(\varepsilon_{ij,1}^{m} + \varepsilon_{ij,1}^{th}) \tag{18}$$

the interaction integral M^l can be expressed as

$$M^l = M^m + M^{th} \tag{19}$$

with some modification, M^m should be defined as [31-32]

$$M^m = \int_A \left\{\sigma_{ij}u_{i,1}^{aux} + \sigma_{ij}^{aux}u_{i,1} - \frac{1}{2}(\sigma_{ik}\varepsilon_{ik}^{aux} + \sigma_{ik}^{aux}\varepsilon_{ik}^{m})\delta_{1j}\right\} q_{,j}\, dA + \int_A \left\{\sigma_{ij}\left(s_{ijkl}^{tip} - s_{ijkl}(x)\right)\sigma_{kl,1}^{aux}\right\} q\, dA \tag{20}$$

Also, for plane stress states

$$\sigma_{33}\varepsilon_{33}^{aux} = \sigma_{33}^{aux}\varepsilon_{33}^{m} = 0 \tag{21}$$

and

$$\sigma_{33}\varepsilon_{33}^{aux} = 0 \quad and \quad \sigma_{33}^{aux}\varepsilon_{33}^{m} \neq 0 \tag{22}$$

$$\sigma_{33} = \nu_{31}\sigma_{11} + \nu_{32}\sigma_{22} - E_{33}\alpha_{33}\Delta T \tag{23}$$

In addition, the thermal interaction integral is expressed as

$$M^{th} = \int_A \left\{\sigma_{ij}^{aux}\varepsilon_{ij,1}^{th}\right\} qdA = \int_A \left\{\sigma_{ii}^{aux}[\lambda_{ii,i}(\Delta T) + \lambda_{ii}T_{,1}]\right\} qdA \tag{24}$$

The relationship between J-integral and the mode I and mode II SIFs can be written as [31-32]:

$$G = J = c_{11}K_I^2 + c_{12}K_IK_{II} + c_{22}2K_{II}^2 \tag{25}$$

with

$$c_{11} = -\frac{a_{22}}{2}Im\left(\frac{\mu_1+\mu_2}{\mu_1\mu_2}\right) \tag{26}$$

$$c_{12} = -\frac{a_{22}}{2}Im\left(\frac{1}{\mu_1\mu_2}\right) + \frac{a_{11}}{2}\,Im\,(\mu_1\mu_2) \tag{27}$$

$$c_{22} = \frac{a_{11}}{2}Im(\mu_1 + \mu_2) \tag{28}$$

The affection of two superimposed fields should be defined as [33]

$$M^l = 2c_{11}K_I^{aux}K_I + c_{12}(K_I^{aux}K_{II} + K_{II}^{aux}K_I) + 2c_{22}K_{II}^{aux}K_{II} \tag{29}$$

Substituting $K_I^{aux} = 1, K_{II}^{aux} = 0$ and $K_I^{aux} = 0, K_{II}^{aux} = 1$ into Eq. (29), gives:

$$\begin{Bmatrix} M_1^l = 2c_{11}K_I + c_{12}K_{II} & (K_I^{aux} = 1\ and\ K_{II}^{aux} = 0) \\ M_2^l = c_{12}K_I + 2c_{22}K_{II} & (K_I^{aux} = 0\ and\ K_{II}^{aux} = 1) \end{Bmatrix} \tag{30}$$

3.3. Auxiliary Fields

The general solution of the stress function $\phi = \phi\left(x_1 + \mu x_2\right)$ for orthotropic FGMs, distinguish equation can apply in tip of discontinuity [30]

$$a_{11}^{tip}\mu^{tip4} - 2a_{16}^{tip}\mu^{tip3} + \left(2a_{12}^{tip} + a_{66}^{tip}\right)\mu^{tip2} - 2a_{26}^{tip}\mu^{tip} + a_{22}^{tip} = 0 \tag{1}$$

the roots μ_i^{tip} of equation (31) are unreal that could express as conjugate pairs configuration, $\mu_1^{tip}, \bar{\mu}_1^{tip}$ *and* $\mu_2^{tip}, \bar{\mu}_2^{tip}$ [30].

a_{ij}^{tip} and μ_k^{tip} are the properties of material at the tip of crack, calculated by Eq .(31), respectively.(X_1, X_2) are global coordinate system components, (x_1, x_2) are local crack tip system components and the local crack tip polar coordinate system (r, θ) can be expressed by $x_1 + ix_2 = re^{i\theta}$, as depicted in Figure 2.

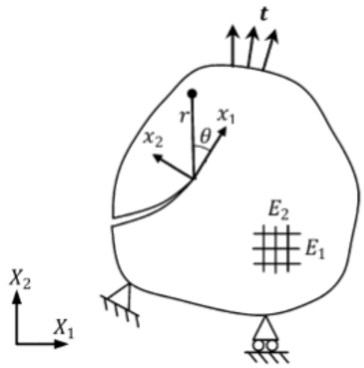

Fig. 1 An Orthotropic cracked FGM.

4. EXTENDED FINITE ELEMENT METHOD (X-FEM)

The satisfaction for a function g_k to verify (PU) condition in XFEM in the problem domain Ω_{PU} is

$$\sum_{k=1}^{m} g_k(x) = 1 \quad (x \in \Omega_{PU}) \tag{32}$$

In addition, PU function fulfills the relevant condition for an arbitrary function ψ

$$\sum_{k=1}^{m} g_k(x)\psi(x) = \psi(x) \quad (x \in \Omega_{PU}) \tag{33}$$

The shape functions of isoparametric finite element, N_i, fulfill Eq. (32), those functions are used as regional enhancement functions that give useful field through domain Ω_{enr}

$$\psi(x) = \sum_{i\in N_{enr}} N_i(x)\psi(x) \quad (x \in \Omega_{enr}) \tag{34}$$

Where N^{enr} defines enriched nodes set and a_i are additional degree of freedoms. Producing of single function ψ in a set of M enrichment functions, that give an analytical solution ϕ,

$$M = \{\psi_1, \psi_2, \dots, \psi_m\} \tag{35}$$

Results in producing of PU technique (44) for generating ϕ

$$\phi = \sum_{i\in N_{enr}} N_i(x)\left(\sum_{m\in M} \psi_m(x) a_{im}\right) \quad (x \in \Omega_{enr}) \tag{36}$$

The displacement of the domain are found from enriched XFEM and the standard FEM:

$$\boldsymbol{u} = \boldsymbol{u}^{FEM} + \boldsymbol{u}^{XFEM} \tag{2}$$

where $\boldsymbol{u}^{XFEM}$ can be defined as

$$\boldsymbol{u}^{XFEM} = \boldsymbol{u}^{tip} + \boldsymbol{u}^{He} \tag{38}$$

$\boldsymbol{u}^{tip}$ and $\boldsymbol{u}^{He}$ are the displacements coincided with the tip of crack enhancement and Heavy-set enhancement regions, sequentially.

4.1. Heavy-Set (Heaviside) Functions for Cracks

XFEM represents discontinuity through definite element via using Heavy-set enrichment function,

$$H(\xi) = \begin{cases} 1 & \forall \xi > 0 \\ -1 & \forall \xi < 0 \end{cases} \tag{39}$$

The sign distance function $\xi(x)$ in point $\boldsymbol{x}$ are expressed from its projection $\boldsymbol{x}_\Gamma$ on crack, as illustrated in Figure (3).

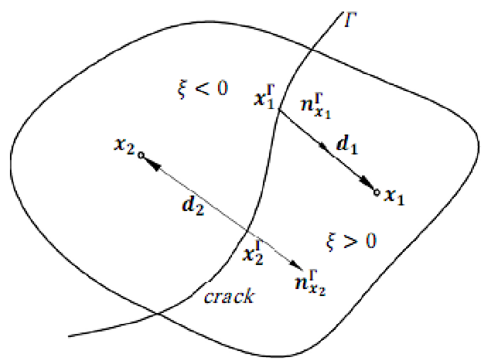

Fig. 3 Representation of the sign distance function [29].

4.2. Crack-Tip Enhancements (Enrichments)

Application of the crack tip enhancements for precise representation of (σ) and (u) terms round tip of crack:

$$\boldsymbol{u}^{Tip} = \sum_{i\in N^{tip}} N_i(\boldsymbol{x})\left(\sum_{k\in F} f_k(\boldsymbol{x})\hat{\boldsymbol{b}}_{ik}\right) \tag{40}$$

F is tip enrichment functions term,

$$F = \{f_1, f_2, \dots, f_m\} \tag{41}$$

In isotropic FGMs, the enrichment functions of the homogeneous materials are used to enrich the solution[13]:

$$F = \left\{\sqrt{r}\,\sin\left(\frac{\theta}{2}\right), \sqrt{r}\,\cos\left(\frac{\theta}{2}\right), \sqrt{r}\,\sin\left(\frac{\theta}{2}\right)\sin(\theta), \sqrt{r}\,\cos\left(\frac{\theta}{2}\right)\sin(\theta)\right\} \tag{42}$$

For orthotropic FGMs, the enrichment functions of non-homogeneous materials that used to enrich the solution in [18,31-32] are applied in the current research.

5. NUMERICAL INTEGRATION

The optimal meshing and suitable numeral of elements round crack tip are selected. Gaussian technique (Q4) is applied for integration rather than use sub-triangulation method, to reduce time cost and to remove non-coincide integrated points about crack surfaces and tips with give same level of accuracy. Therefore, numerical integrity is adopted as a grid with a 2 × 2 Gaussian quadrature rule for whole domain.

6. NUMERICAL EXAMPLE

Consider (FGCM) plate with slanted crack *(2a, a/W=0.1, L/W=1.0)* under thermal loadings, illustrated in Figure 4. This example is adopted to check the predicted SIFs for thermal loadings with available solutions results in the literature. Thermos load applies (Figure 4a) in while the bottom and top edges are bound. Another load case supposes as corresponded mechanical load of thermal load (Figure 4b).

The following material properties for an isotropic case are considered

$$E^0 = 1.0, \quad \upsilon = 0.3 \tag{43}$$

$$E(X_1) = E^0 e^{\beta X_1}, \alpha(X_1) = \alpha^0 e^{\delta X_1}, \upsilon(X_1) = \upsilon_0 \tag{44}$$

The nonhomogenity parameter βa equals to 0.5 and the exponentially changes of mechanical and thermal parameters are supposed over (X_1) axis,

In addition, the following material properties for an orthotropic case are considered

$$E_{11}^0 = 10^4\ MPa, \qquad E_{22}^0 = 10^3\ MPa,$$

$$\nu_{12}^0 = 0.3, \qquad G_{12}^0 = 1216\ MPa \tag{45}$$

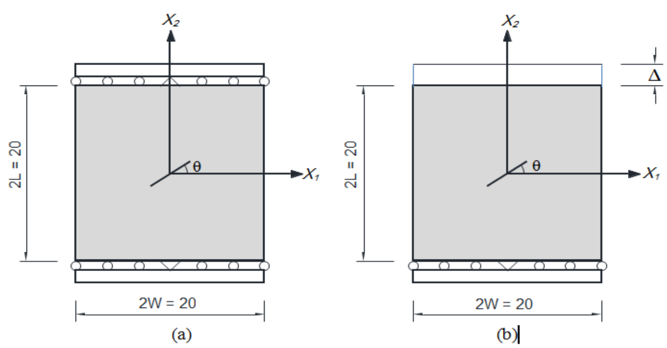

Fig. 4 Example Configuration Under

(a) Thermal, and (b) Mechanical Loads.

and the variations are written as,

$$E_{11}(X_1) = E_{11}^0 e^{\beta X_1}, \quad E_{22}(X_1) = E_{22}^0 e^{\beta X_1},$$

$$\nu_{12}(X_1) = \nu_{12}^0, \qquad G_{12}(X_1) = G_{12}^0 e^{\beta X_1} \tag{46}$$

$$\alpha_{11}(X_1) = \alpha_{11}^0 e^{\delta_1 X_1}, \quad \alpha_{22}(X_1) = \alpha_{22}^0 e^{\delta_2 X_1} \tag{47}$$

In addition, equivalent thermal and mechanical loadings are

$$(\varepsilon_{11})_{th} = (\varepsilon_{22})_{th} = -\alpha(X_1)\Delta\theta(X_1) = 1.0 \tag{48}$$

$$(\varepsilon_{22})_{mech} = \bar{\epsilon} = \Delta/2L = 1.0 \tag{49}$$

As shown in Figure 5, the current paper take a similar mesh of [29] in order to compare and to study the perform of Gauss quadrature rule (Q4) against using sub- triangular rule that used in the reference XFEM model (comparison is depicted in Table 1).

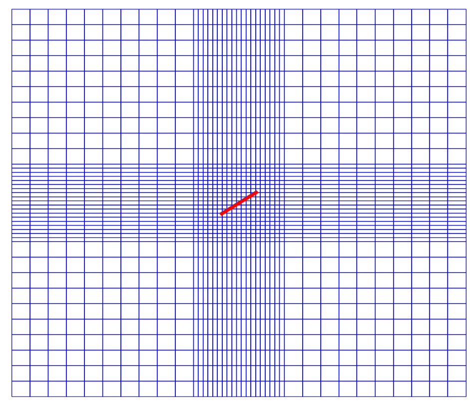

Fig. 5 Mesh of the Square Plate.

In addition, Table 1 illustrates comparison between the current work (XFEM model with 1600 nodes- Gauss quadrature rule (Q4)) and the reference conventional finite element model [26]. Also, in Table 2, results of the an orthotropic FG model [25] at 5336 DOFs and current solution depicts the efficiency of XFEM in comparison with traditional numerical techniques. Cleraly, Good agreements are noted in all values.

TABLE 1. Normalized SIFs for Isotropic FGM Under Thermal Load.

θ	Normalized K_I						Normalized K_{II}					
	left			right			left			right		
	[29]	[26]	Present work	[29]	[26]	Present work	[29]	[26]	Present work	XFEM	[26]	Present work
0	0.663	0.665	0.665	1.419	1.423	1.425	0.000	0.000	0.000	0.000	0.000	0.000
18	0.616	0.610	0.608	1.273	1.283	1.277	0.213	0.211	0.211	0.337	0.344	0.342
36	0.451	0.455	0.461	0.930	0.923	0.920	0.354	0.362	0.369	0.562	0.549	0.541
54	0.249	0.245	0.251	0.480	0.488	0.485	0.391	0.394	0.394	0.536	0.532	0.538
72	0.063	0.058	0.064	0.144	0.145	0.141	0.245	0.266	0.256	0.344	0.314	0.328

TABLE 2. Normalized SIFs for Orthotropic FGM.

θ	Normalized SIF	Left [29]	Left [25]	Left Present work	right [29	right [25	right Present work
0	K_I/K_0	0.659	0.6663	0.662	1.429	1.427	1.447476
	K_{II}/K_0	0	0	0	0	0	0
18	K_I/K_0	0.592	0.599	0.619	1.329	1.322	1.309827
	K_{II}/K_0	0.277	0.243	0.246	0.246	0.215	0.220695
36	K_I/K_0	0.426	0.416	0.429	1.01	1.019	1.017028
	K_{II}/K_0	0.398	0.415	0.400	0.411	0.408	0.413268
54	K_I/K_0	0.194	0.18	0.195	0.587	0.599	0.589499
	K_{II}/K_0	0.435	0.438	0.435	0.443	0.447	0.443941
72	K_I/K_0	0.027	0.006	0.027904	0.216	0.217	0.215433
	K_{II}/K_0	0.27	0.282	0.270613	0.305	0.29	0.303858

It can be noted in Figure 6-7, where the biggest energy release rate relates at horizontal crack. Also, in Figure 7, Clearly there is good agreement between the current work and reference [29]. For further check out the effect of the radius of J integral and enrichment domain size on normalized SIFs is illustrated in Figure 8 a-b. In Figure (6-8), It is clear that J-integral domain value significantly has not influence the current study. It is clear that the size of J-integral domain significantly does not affects the solution. Generally, energy release rate decreased when crack angles increased.

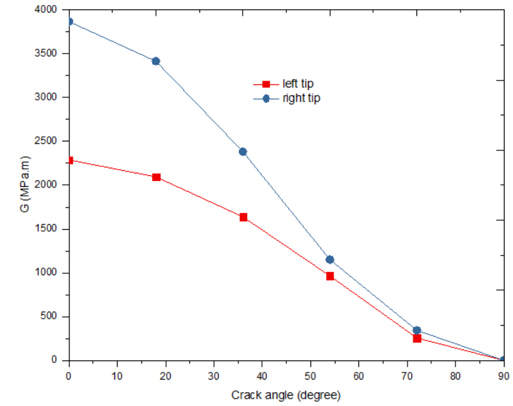

Fig. 6 Energy Release Rate in Isotropic FGM.

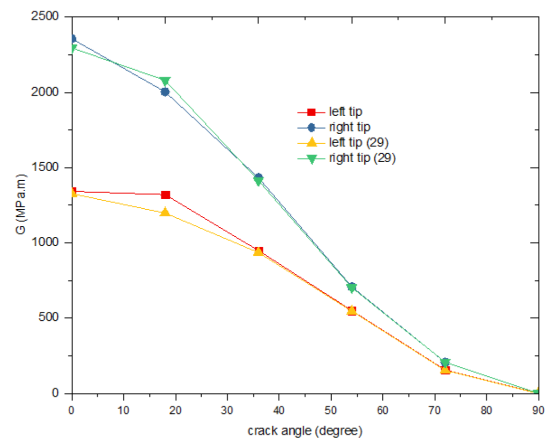

Fig. 7 Energy Release Rate in Orthotropic FGM.

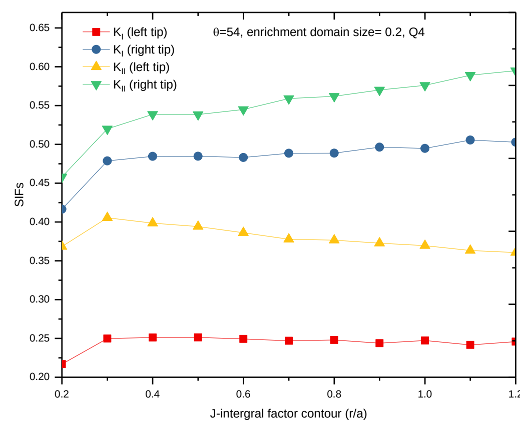

(a)

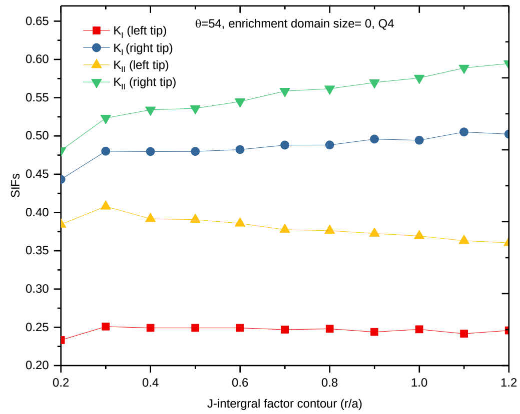

(b)

Fig.8 a-b Normalized SIFs Versus Radius of J-Integral for Isotropic FGM

7. CONCLUSIONS

XFEM are adopted for crack analysis in FGMs under thermal load. Crack tip enhancements are applied to give behavior of stress field in discontinuity tips. Mixed-mode SIFs are calculated in isotropic and anisotropic FG Plate. Gaussian technique (Q4) is applied to numerical integration rather than used sub-triangulation method to reduce time cost and to remove non-coincide integrated points about crack surfaces and tips with give same level of accuracy. It is clear that Gauss quadrature rule (Q4) gives approximately the same accuracy of sub-triangulation technique at same DOFs; this gives an important explanation, that the enrichments functions play a big and prominent role on the results. In addition, comparisons are implemented between the proposed method results and the reference results available in the literature. Energy release rate decreased when crack angles increased. In addition, it can be noted where the biggest energy release rate relates at horizontal crack . Good agreement and high convergence are noted.

8. REFERENCE

[1]. I. Shiota and Y. Miyamoto, Functionally graded materials, Proceedings of the 4th International Symposium on Functionally Graded Materials, October 21–24, Tsukuba, Japan, 1996.

[2]. Jin, Z.-H., An Asymptotic Solution of Temperature Field in a Strip of a Functionally Graded Material. International Communication in Heat and Mass Transfer, 2002. 29: p. 887–895.

[3]. Ootao, Y., and Tanigawa, Y., Transient Thermoelastic Problem of Func-tionally Graded Thick Strip Due to Nonuniform Heat Supply. Composite Structures, 2004. 63: p. 139–146.

[4]. Zhang Zhengyu (Jenny)., and G., H, P., Cohesive zone modeling of dynamic failure in homogeneous and functionally graded materi-als. International Journal of Plasticity 2005. 21(6): p. 1195–54.

[5].El-Hadek Medhat, A., and Tippur Hareesh, V., Dynamic fracture behavior of syntactic epoxy foams: optical measurements using coherent gradient sensing. Optic and Lasers in Engineering, 2003. 40(4): p. 353-369.

[6].Arun, S., and Nitesh, J., Dynamic damage growth in particle-reinforced graded materials. International Journal of Impact Engineering, 2004. 30(7): p. 777–803.

[7]. Yao, X.F., Xu, W., Arakawa, K., Takahashi, K., and Mada, T., Dynamic optical visualization on the interaction between propagating crack and stationary crack. Optic and Lasers in Engineering, 2005. 43(2): p. 195–207.

[8]. El-Hadek Medhat, A., and Tippur Hareesh, V., Dynamic fracture parameters and constraint effects in functionally graded syntactic epoxy foams. International Journal of Solids and Structure, 2003. 40(8): p. 1885–906.

[9]. Marur, P.R., and Tippur, H.V. , Dynamic response of bimaterial and graded interface cracks under impact loading. International Journal of Fracture Mechanics, 2000. 103(1): p. 95–109.

[10]. Kawasaki, A., and Watanabe, R., Thermal Fracture Behavior of Metal/Ceramic Functionally Graded Materials. Engineering Fracture Mechanics, 2002. 69: p. 1713–1728.

[11]. F. Delale and F. Erdogan, The crack problem for a non-homogeneous plate, J. Appl. Mech., vol. 50, no. 3, pp. 609–614, 1983.

[12]. J.E. Dolbow, and M. Gosz, On the computation of mixed-mode stress intensity factors in functionally graded materials, Int. J. Solids Struct., vol. 39, pp. 2557–2574, 2002.

[13]. B.N. Rao, and S. Rahman, Mesh-free analysis of cracks in isotropic functionally graded materials, Eng. Fract. Mech., vol. 70, pp. 1–27, 2003.

[14]. J.-H. Kim, and G. H. Paulino, An accurate scheme for mixed-mode fracture analysis of functionally graded materials using the interaction integral and micromechanics models, Int. J. Numer. Methods Eng., vol. 58, pp. 1457–1497, 2003.

[15]. J.-H. Kim, and G.H. Paulino, Consistent formulations of the interaction integral method for fracture of functionally graded materials, J. Appl. Mech., vol. 72, pp. 351–364, 2005.

[16]. K.Y. Dai, G.R. Liu, K.M. Lim, X. Han, and S.Y. Du, A meshfree radial point interpolation method for analysis of functionally graded material (FGM) plates, Comput. Mech., vol. 34, pp. 213–223, 2004.

[17]. J. Sladek, V. Sladek, and C. Zhang, A meshless local boundary integral equation method for dynamic anti-plane shear crack problem in functionally graded materials, Eng. Anal. Bound. Elem., vol. 29, pp. 334–342, 2005.

[18]. H. Khazal, H. Bayesteh, S. Mohammadi, S.S. Ghorashi, and A. Ahmed, An extended element free Galerkin method for fracture analysis of functionally graded materials, Mech. Adv. Mater. Struct. 23 (2015) 513–528.

[19]. Hasselman, D.P.H., and Youngblood, G.E., Enhanced thermal stress resistance of structural ceramics with thermal conductivity gradient. Journal of American Ceramic Society, 1978. 61: p. 49-52.

[20]. Abotula S., Kidane A., Chalivendra V.B., and Shukla A, Dynamic curving cracks in functionally graded materials under thermo-mechanical loading. International Journal of Solids and Structures, 2012.

[21]. Noda N., and Jin Z.H., Steady thermal stress in an infinite nonhomogeneous elastic solid containing a crack. Journal of Thermal stresses, 1993. 16: p. 181-196.

[22]. EI-Borgi S., Erdogan F., and Hatira, F.B., Stresses intensity factors for an interface crack between a functionally graded coating and a homogeneous substrate. International Journal of Fracture, 2003. 123: p. 139–162

[23]. EI-Borgi S., Erdogan F., and Hidri L., A partially insulated embedded crack in an infinite functionally graded medium under thermal-mechanical loading. International Journal of Engineering Science, 2004. 42: p. 371–393.

[24]. Ding, S.-H., and Li, X., Thermal stress intensity factors for an interface crack in a functionally graded layered structures. Archive of Applied Mechanics, 2011. 81: p. 943–955.

[25]. Kim, J.-H., and Amit, K.C., A Generalized Interaction Integral Method for the Evaluation of the T - Stress in Orthotropic Functionally Graded Materials Under Thermal Loading. Journal of Applied Mechanics, 2008. 75.

[26]. Amit, K.C., and Kim, J-H., Interaction integrals for thermal fracture of functionally graded materials. Engineering Fracture Mechanics 2008. 75: p. 2542–2565.

[27]. Serkan Dag, E.E.A., and Bora Yildirim, Computation of thermal fracture parameters for orthotropic functionally graded materials using J k-integral. International Journal of Solids and Structures, 2010. 47: p. 3480–3488.

[28]. Dag, S., Thermal fracture analysis of orthotropic functionally graded materials using an equivalent domain integral approach. Engineering Fracture Mechanics 2006. 73: p. 2802–2828.

[29]. S.S. Hosseini, H. Bayesteh, and S. Mohammadi, Thermo-mechanical XFEM crack propagation analysis of functionally graded materials. Materials Science & Engineering A 561 (2013) 285–302.

[30]. Lekhnitskii, S.G., Theory of an anisotropic elastic body. Holden-Day: San Francisco, 1963.

[31]. Jeong-Ho Kim, Mixed mode crack propagation in functionally graded materials, Ph.D thesis, University of Illinois at Urbana-Campaign, 2000.

[32]. Guo L.C., Guo F.N., Yu H.J., and Zhang L., An interaction energy integral method for nonhomogeneous materials with interfaces under thermal loading, Int. J. Solids Struct. **49**, 355–365 (2012).

[33]. S.S. Wang, J.F. Yau, and H.T. Corten, A mixed-mode crack analysis of rectilinear anisotropic solids using conservation laws of elasticity, Int. J. Fract. 16 (1980) 247–259.